2.L

Nuclear Physics A294 (1978) 473–491; © *North-Holland Publishing Co., Amsterdam*

NEUTRAL CURRENT AND THE NUCLEAR SCATTERING OF REACTOR ANTINEUTRINOS

H. C. LEE

Atomic Energy of Canada Limited, Chalk River Nuclear Laboratories, Chalk River, Ontario, Canada K0J 1J0

Received 27 June 1977

Abstract: Expressions are derived for evaluating the integrated inelastic cross section, $\bar{\sigma}_\nu$, for the nuclear scattering of reactor antineutrinos in terms of experimentally determined B(M1) values and Gamow-Teller matrix elements. These expressions are used to compute $\bar{\sigma}_\nu$ for many nuclear transitions.

1. Introduction

The history of experiments on neutrino-induced reactions extends back more than two decades. The early experiments were concerned with establishing the existence of neutrinos [1]), and later the existence of two different types of neutrinos [2]), the conservation of lepton numbers and the search for intermediate bosons [3,4]). In terms of the current-current weak interaction, the neutrino had been, until quite recently, only associated with the charged current. Although the existence of weak neutral currents was predicted in the late fifties [5]) and early sixties [6]), the argument was considered to be sufficiently convincing only after the concept of spontaneous symmetry breaking [7]) was used in unifying the weak and electromagnetic interactions [8–10]).

In the SU(2) × U(1) unified theory of Salam [8]) and Weinberg [9]), the lepton neutral current is related to the well known V − A (charged) current by a rotation in "isospin" space. The nucleon neutral current has an additional term proportional to the electromagnetic (EM) current

$$J_\mu^{(0)} = J_\mu^{V-A(0)} - 2J_\mu^\gamma \sin^2\theta_W, \tag{1}$$

where J_μ^{V-A} is the V − A current and J_μ^γ is the EM current. The Salam-Weinberg angle θ_W describes the mixing of the third component of the SU(2) isovector lepton field with the U(1) photon field and appears as a free parameter in the theory. Neutral current events were first identified [11]) experimentally in 1973. Since then we have witnessed a very significant growth in the number of neutrino related experiments [12]). To date all neutral current measurements have been sensitive to the parameter $x = \sin^2\theta_W$, and the value $x \approx 0.35$ is in agreement with the interpretation of almost all results. However, results of recent experiments [13]) on parity-violating neutral current effects in atomic bismuth are not in agreement with predictions of the Salam-Weinberg theory.

Interestingly, another important aspect of (1), which is unrelated to the adjustable Salam-Weinberg angle, namely that the axial neutral current is simply related to the axial charged current by a rotation in isospin space [10]), has so far not been directly tested. In principle the ideal test of this statement would be the measurement of the cross section for the elastic scattering of low-energy neutrinos by the nucleus. However, the detection of either the final neutrino or the recoiling nucleus in an elastic scattering will probably remain impracticable in the foreseeable future. The measurement of the inelastic cross section is more promising since one might hope to detect signatures following the decay of the excited nuclear state. Fig. 1 illustrates idealized systems for the kind of experiment under consideration. The nuclear matrix element for the inelastic scattering (ν, ν') process is related to the Gamow-Teller matrix elements for the $\beta^{\pm}$ decays by Clebsch-Gordon coefficients for the appropriate isospin transformations. In fig. 1a the ground state of the target nucleus

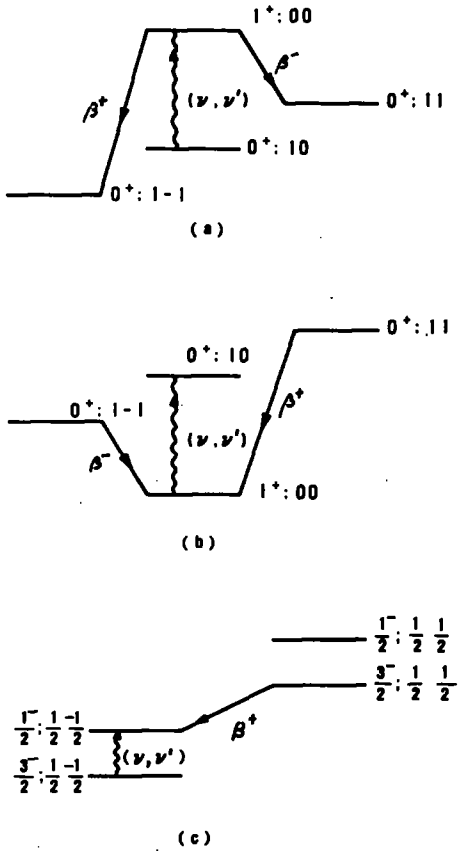

Fig. 1. Schematic relationship between the (ν, ν') reaction and $\beta^{\pm}$ decays. (a) The initial state of (ν, ν') is the $T_3 = 0$ member of an isotriplet. (b) The final state of (ν, ν') is the $T_3 = 0$ member of an isotriplet. (c) The states involved are two isodoublets. The notation $J^{\pi}; TT_3$ is used for the spin-parity and the isospin of the nuclear states. Spin-parity assignments are arbitrary.

is the $T_3 = 0$ member of an isospin triplet. In fig. 1b the excited state is the $T_3 = 0$ member of the isospin triplet. Fig. 1c shows yet another system involving only isospin doublets.

The neutrino disintegration of the deuteron is another variation of (ν, ν'). This reaction is of special interest since the measurement [14]) of the cross section has been underway for some time and presumably a firm result will be forthcoming in the near future.

There are other types of experiments pertaining to neutral currents in the nucleus. Of particular interest are those which seek to measure parity mixings [15]) in nuclear states. Since strong and electromagnetic interactions conserve parity, such mixings must be attributed to the weak interaction among nuclei. In general the sensitivity in such measurements is greater than could be expected in (ν, ν') experiments. However, because parity mixing is very sensitive to details of the nuclear structure and arises from charged as well as neutral currents the analysis of the experimental result would be very complicated. In contrast the measurement of (ν, ν') cross sections is much harder but the result could provide clear-cut answers to questions related to the neutral current. We believe these two types of experiments should be viewed as mutually complementary.

The excitation of nuclear states by reactor antineutrinos was first discussed by Gershtein *et al.* [16]). The cross section computed for ^{7}Li appears to be too large, however. More recently the (ν, ν') reaction was discussed, in the context of a unified treatment of the semi-leptonic weak and electromagnetic interactions with nuclei, in a series of papers [17]) by O'Connell, Donnelly, Walecka and co-workers. The present paper will be concerned with the (ν, ν') reaction only, but the treatment is in greater detail for reactor antineutrinos. It is written with two goals in mind. The first is to derive some useful but simple expressions for the (ν, ν') cross section. This is carried out in sect. 2. In sect. 3 we pursue the second goal of using existing nuclear data and expressions derived in sect. 2 to compute and set up a catalog of predicted (ν, ν') cross sections for nuclear targets. Sect. 4 is a summary.

2. Formalism

2.1. GENERAL EXPRESSION FOR THE (ν, ν') CROSS SECTION

The general expression for the (ν, ν') cross section can be found in the literature [17]). For completeness, a brief but self-contained derivation is provided in appendix A. The result † is

$$\frac{d\sigma_{i\to f}}{d\Omega_\nu} = \frac{2}{\pi}\frac{2J_f+1}{2J_i+1} G_w^2(\varepsilon_\nu - \Delta)^2 \cos^2\tfrac{1}{2}\theta \sum_{\lambda=0} \left| M_\lambda - \frac{\Delta}{q} L_\lambda \right|^2 + [\tan^2\tfrac{1}{2}\theta - q_\mu^2/2q^2]$$
$$\times \sum_{\lambda=1} (|T_\lambda^{el}|^2 + |T_\lambda^{mag}|^2) \pm \tan\tfrac{1}{2}\theta[\tan^2\tfrac{1}{2}\theta - q_\mu^2/q^2] \sum_{\lambda=1} \mathrm{Re}\,(T_\lambda^{el} T_\lambda^{mag*}), \qquad (2)$$

† We use $c = \hbar = 1$.

where G_w is the weak coupling constant; ε_ν is the initial neutrino energy; Δ is the nuclear excitation energy; θ is the neutrino scattering angle; q^2 is the three-momentum transfer squared; $q_\mu^2 = \Delta^2 - q^2$; M_λ, L_λ, $T_\lambda^{\rm el}$ and $T_\lambda^{\rm mag}$ are respectively the charge, longitudinal, transverse electric and transverse magnetic nuclear transition matrix elements and are functions of q; λ is the multipolarity. The interference term has a $+$ $(-)$ sign for neutrino (antineutrino) scattering.

In (2), rather than using the notation commonly used in the study of nuclear β-decay, we follow Donnelly *et al.* [17]) and use the notation which is more prevalent in the study of electron scattering. These authors advocate a unified treatment of nuclear semi-leptonic reactions of which β-decay, electron scattering, μ-capture and neutrino scattering are special cases.

2.2. SPECIAL CASE FOR LOW-ENERGY NEUTRINOS

We now restrict the discussion to neutrinos for which $\varepsilon_\nu \ll M$, where M is the nucleon mass. This is the case for reactor antineutrinos, of which only a very minute fraction has an energy exceeding 4 MeV.

The leading term in the nuclear vector-current is the identity and does not contribute to (ν, ν'); next order terms which are proportional to $q/M \leqq 2/M \ll 1$ will be ignored. The leading axial-current term,

$$J_{\rm axial} = \tfrac{1}{2} g_{\rm A} \sigma \tau_3, \tag{3}$$

where $g_{\rm A}$ is the ratio of the axial to vector weak coupling constants, is the leading term contributing to (ν, ν'). From (A.7) and (3) we find that

$$\begin{aligned} \langle {\rm f}||(L_1)_{\rm axial}||{\rm i}\rangle &= -\sqrt{\tfrac{1}{2}}\langle {\rm f}||(T_1^{\rm el})_{\rm axial}||{\rm i}\rangle \\ &= -ig_{\rm A}\sqrt{\frac{1}{12\pi}}\langle {\rm f}||\tfrac{1}{2}\sigma\tau_3||{\rm i}\rangle, \end{aligned} \tag{4}$$

where $|{\rm i}\rangle$ and $|{\rm f}\rangle$ are respectively the initial and final nuclear states. After substituting (4) into (2), integrating over the neutrino angle, and using the value [18]) $G_w M^2 = 1.03 \times 10^{-5}$, we obtain

$$\sigma_{{\rm i}\to{\rm f}}(\varepsilon_\nu) = 4.2 \times 10^{-45}(\varepsilon_\nu - \Delta)^2 |g_{\rm A}\langle\sigma\tau_3\rangle|^2 \ {\rm cm}^2, \tag{5}$$

where ε_ν and Δ are in units of MeV and $\langle\sigma\tau_3\rangle$ is a shorthand notation for the reduced nuclear matrix element $\langle {\rm i}||\sigma\tau_3||{\rm f}\rangle$. It should be pointed out that when (5) is a valid approximation the scatterings of neutrinos and antineutrinos are indistinguishable. From now on, unless otherwise specified, we shall use the term neutrino to indicate both kinds of particles.

Eq. (5) is the general expression for "allowed" nuclear transitions in low energy (ν, ν'). However, since at the present time there is no monoenergetic neutrino source,

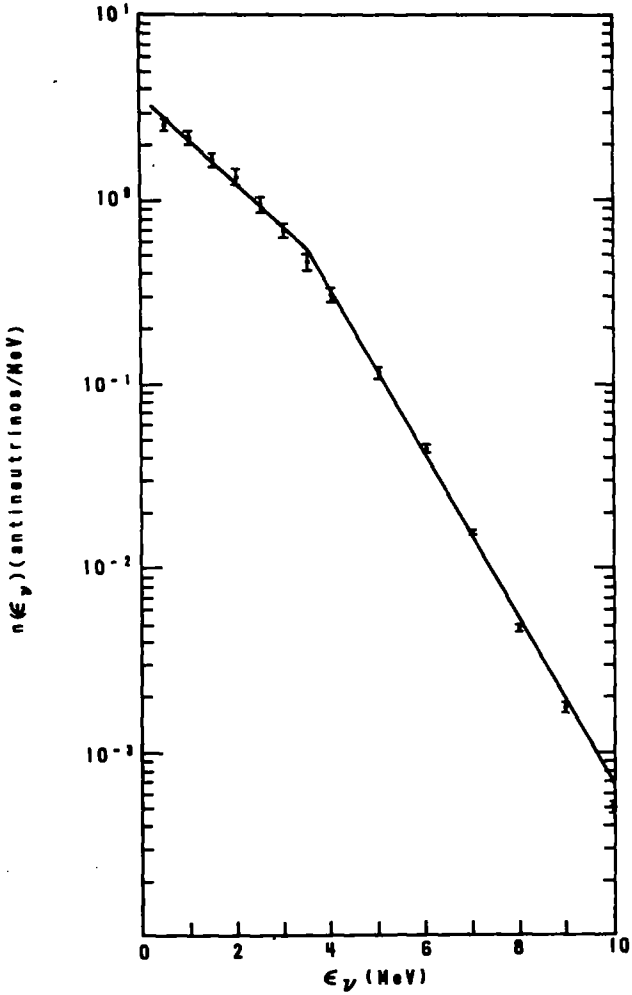

Fig. 2. Antineutrino spectrum of a ^{235}U fission reactor in secular equilibrium calculated by Avignone [19], fitted to two sections of exponentials [see (7)].

the cross section must be integrated over the spectrum, $n(\varepsilon_\nu)$, of the source

$$\bar{\sigma}_\nu(\Delta) \equiv \int_\Delta^\infty \sigma(\varepsilon_\nu) n(\varepsilon_\nu) \mathrm{d}\varepsilon_\nu \Big/ \int_0^\infty n(\varepsilon_\nu) \mathrm{d}\varepsilon_\nu. \tag{6}$$

In the following we consider specifically the reactor as a source of antineutrinos.

The energy spectrum of antineutrinos from ^{235}U fission products in secular equilibrium has been calculated by Avignone [19]. The number of antineutrinos per MeV per fission can be very adequately represented by the simple exponentials

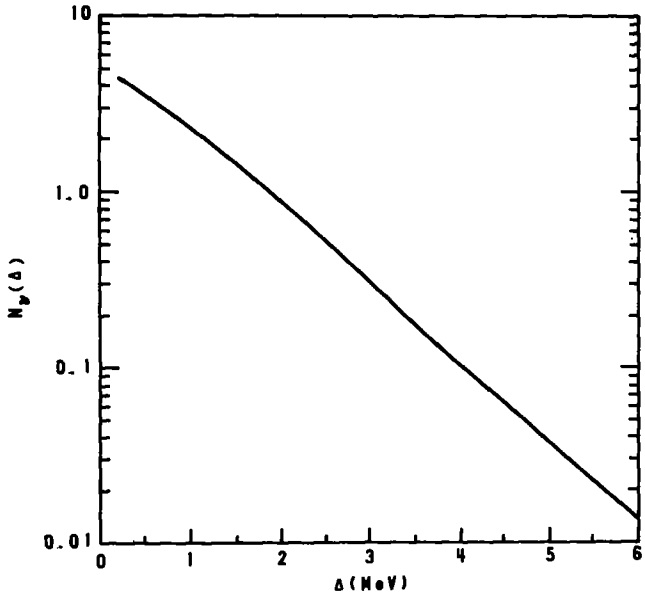

Fig. 3. The function $N_\nu(\Delta)$ defined in (9).

(see fig. 2)

$$n(\varepsilon_\nu) = \begin{cases} 0, & \varepsilon_\nu < 0.20 \\ 3.63\,e^{-0.543\varepsilon_\nu}, & 0.20 \leqq \varepsilon_\nu \leqq 3.4 \\ 17.8\,e^{-1.01\varepsilon_\nu}, & 3.4 < \varepsilon_\nu, \end{cases} \tag{7}$$

where ε_ν is in MeV. The number of antineutrinos per fission given by (7) is 5.9, as compared to the number 6.0 given by Avignone. The 2% difference is due to the artificial cutoff at $\varepsilon_\nu = 0.2$ MeV in (7). Since we do not consider any reaction with $\Delta < 0.2$ MeV this small error is simply rectified by replacing $\int_0^\infty n d\varepsilon_\nu$ by 6.0 in (6). From (6) and (7) we obtain an energy averaged, or mean, cross section for Gamow-Teller transitions:

$$\bar{\sigma}_\nu(\Delta) = 4.2 \times 10^{-45} |g_A \langle \sigma\tau_3 \rangle|^2 N_\nu(\Delta)\ \text{cm}^2, \tag{8}$$

where

$$N_\nu(\Delta) = \begin{cases} 7.54\,e^{-0.543\Delta} - 0.0954[f(0.543) - f(1.01)], & 0.2 \leqq \Delta \leqq 3.4 \\ 5.80 e^{-1.01\Delta}, & \Delta \geqq 3.4, \end{cases} \tag{9}$$

with

$$f(\zeta) = [(3.4-\Delta)^2\zeta^2 + 2(3.4-\Delta)\zeta + 2]/\zeta^2.$$

The function $N_\nu(\Delta)$ is plotted in fig. 3. We see that for a fixed Gamow-Teller matrix

element, $\bar{\sigma}_\nu(\Delta)$ decreases essentially exponentially with increasing Δ. Eqs. (8) and (9) (or fig. 3) are the important results of this section.

2.3. EXTRACTING $\langle\sigma\tau_3\rangle$ FROM GAMOW-TELLER β-DECAY RATES

In (8) the nuclear matrix element $g_A\langle\sigma\tau_3\rangle$ is the only remaining unknown. Because of the Salam-Weinberg assumption that the neutral and charged weak currents from an isospin triplet, this matrix element is related to the corresponding one in (Gamow-Teller) β-decay by a rotation in isospin space. Let T_i (J_i) and T_f (J_f) be the isospins (spins) of the initial and final states respectively and T_{3i} be the third component of the isospin of the initial state, then the Salam-Weinberg assumption implies that

$$\langle i\|\sigma\tau_3\|f\rangle \equiv \langle J_i; T_iT_{3i}\|\sigma\tau_3\|J_f; T_fT_{3i}\rangle$$

$$= \sqrt{2}\,\frac{\langle T_iT_{3i}|T_fT_{3i}10\rangle}{\langle T_iT_{3i}|T_fT_{3i}\mp 1, 1, \pm 1\rangle}\langle J_i; T_iT_{3i}\|\sigma t_\pm\|J_f; T_fT_{3i}\mp 1\rangle, \qquad (10)$$

where $t_\pm \equiv \sqrt{\frac{1}{2}}\tau_\pm$ is the conventional isospin operator used in nuclear β-decay. The last factor in (10) is directly related to the ft value (in sec), of the β-decay by

$$|g_A\langle J_i; T_iT_{3i}\|\sigma t_\pm\|J_f; T_fT_{3i}\mp 1\rangle|^2 = 6165/(ft)_{i\to f}. \qquad (11)$$

The proportional constant 6165 (sec) is determined experimentally [20]).

2.4. EXTRACTING $\langle\sigma\tau_3\rangle$ FROM NUCLEAR M1 TRANSITION RATES

The set of (neutral) Gamow-Teller matrix elements that could be obtained directly from experimental data, as described in the last section is comparatively limited. At the cost of accepting a small inaccuracy, this set of matrix elements can be enlarged considerably, using experimentally known M1 transition rates. The M1 strength, or B(M1) value, in units of (n.m.)^2 for the i $\to$ f transition is †

$$B(\mathrm{M1}; \mathrm{i}\to\mathrm{f}) = \frac{3}{16\pi}|\langle i\|l\tau_3 + (\mu_s - 0.5)\sigma + \mu_\nu\sigma\tau_3\|f\rangle|^2, \qquad (12)$$

where $\mu_s = 0.88$ and $\mu_\nu = 4.70$ are respectively the nucleon isoscalar and isovector magnetic moments. It is well known that unless the transition is very much hindered (for whatever structural reason), $\mu_\nu\langle\sigma\tau_3\rangle$ is the most important term in the M1 matrix element. Introducing a parameter η ($\eta \geqq -1$) such that

$$B(\mathrm{M1}; \mathrm{i}\to\mathrm{f}) \equiv \frac{3}{16\pi}(1+\eta)^2\mu_\nu^2\langle i\|\sigma\tau_3\|f\rangle|^2, \qquad (13)$$

† We ignore contributions from exchange currents, which for strong transitions amount to about 10 % [ref. [21])].

and using the known values for μ_v and g_A [taken here to be [21]) 1.25], we may formally write

$$|g_A\langle i||\sigma\tau_3||f\rangle|^2 = 1.19(1+\eta)^{-2}B(M1; i \to f). \tag{14}$$

Eq. (14) would not be useful if the measured values of η for different transitions varies widely. In fact for those transitions where both B(M1) and $|g_A\langle\sigma\tau_3\rangle|^2$ are known experimentally, the value of η is very regular, as is shown in fig. 4. The

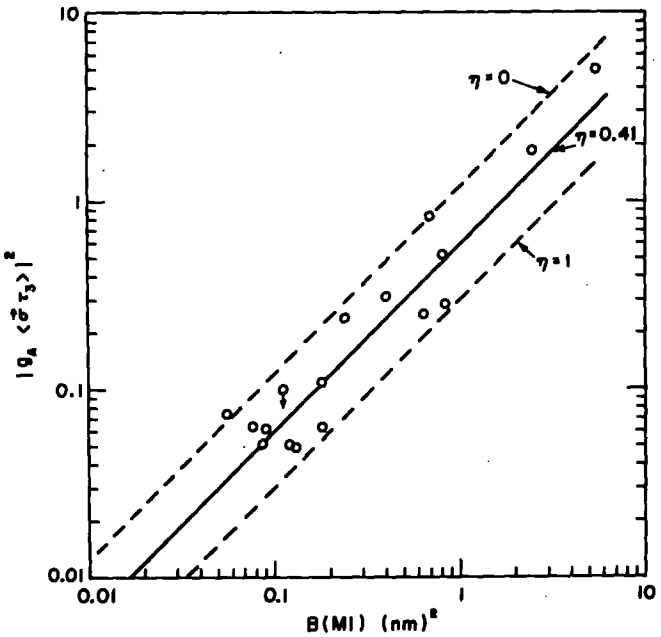

Fig. 4. Correlations between experimental values for $|g_A\langle\sigma\tau_3\rangle|^2$ and B(M1).

individual transitions will be discussed in more detail in subsect. 3.3. Here we only point out that for these transitions η lies within the range $0 \lesssim \eta < 1$. If we use the approximate mean value of $\eta = 0.41$ and predict the Gamow-Teller matrix element from (14), the rms error for the cases of known matrix element is 41 %. This is quite a remarkable result considering that the B(M1) values span two orders of magnitude. We thus adopt the value $\eta = 0.41$ from which follows the empirical relation

$$|g_A\langle i||\sigma\tau_3||f\rangle|^2 \approx 0.60B(M1; i \to f). \tag{15}$$

The B(M1) value is related to the (partial) decay width Γ (in eV), or the mean lifetime τ (in psec), of the $|f\rangle$ state by

$$B(M1) = 86.2\Delta^{-3}\Gamma = 0.0568\Delta^{-3}\tau^{-1}, \tag{16}$$

where Δ (in MeV) is the excitation energy of $|f\rangle$.

2.5. NEUTRINO-DISINTEGRATION OF THE DEUTERON

The (ν, ν') cross sections could also be calculated directly from nuclear wave functions. For our present purpose, which is to confirm or refute the Salam-Weinberg theory with respect to the axial neutral current in the nucleus, such a calculation is warranted only in cases when the wave functions are well known. One of very few such cases is the neutrino-disintegration of the deuteron. This case is of special interest because of the low threshold energy (2.22 MeV) and the large M1 transition matrix element, both of which are favourable conditions for a large cross section. It is also the only case in which a measurement of the cross section is known to be in progress [14]). The cross section has previously been calculated by Ahrens and Lang and by others [22]). In view of the special importance of this case, and the fact that the antineutrino spectrum has been updated since the earlier calculations, we feel it is important to re-do the calculation using the latest antineutrino spectrum [19]). For completeness, details of the calculation is given in appendix B. The result is

$$\frac{\mathrm{d}\bar{\sigma}_\nu}{\mathrm{d}E_\mathrm{r}} = 7.64\times10^{-44}\,\frac{E_\mathrm{r}^{\frac{1}{2}}N_\nu(B+E_\mathrm{r})}{(E_\mathrm{s}+E_\mathrm{r})(B+E_\mathrm{r})}\ \mathrm{cm}^2\cdot\mathrm{MeV}^{-1}, \tag{17}$$

where E_r is the reduced, or relative kinetic energy of the final neutron and proton, $B = 2.22$ MeV, $E_\mathrm{s} = 0.0738$ MeV and the function N_ν is the effective neutrino number given in (9). The appearance of the extra variable E_r is due to the fact that in the present case there are three particles (p, n and ν') in the final state, one more than in cases considered in previous sections.

3. Results and discussion

3.1. CRITERIA FOR SELECTING REACTIONS

Our criteria for selecting the reactions for which we calculate $\bar{\sigma}_\nu$ are the following:

(i) To ensure a relatively large $\bar{\sigma}_\nu$, we require that $|g_\mathrm{A}\langle\sigma\tau_3\rangle| \geqq 0.05$.

(ii) For the same reason we cut Δ off at 4 MeV, since above this energy $N_\nu(\Delta)$ becomes too small.

(iii) The $\bar{\sigma}_\nu$ for a great majority of the reactions would have to be measured by detecting the γ-decay of the final nuclear state following excitation by (ν, ν'). For these reactions we further impose a low-energy cut-off of Δ at about 600 keV to avoid the energy region in which the γ-ray backgrou ıd level is expected to be the highest.

Criterion (ii) excludes excitation to all so-called giant M1 states except the one in ^{6}Li; in most nuclei the giant M1 strength lies in the 10–15 MeV region. These considerations also effectively exclude reactions involving nuclei with A (atomic mass) $\gtrsim 100$ because in these nuclei the M1 strength function in the 600–4000 keV region is essentially unknown.

TABLE 1

Catalogue of targets ($A < 100$) for the ($\bar{\nu}$, $\bar{\nu}'$) reaction

Reaction number	Target nucleus	Initial → final states [a])	Exc. energy Δ (keV)	$\lvert g_A\langle\sigma\tau_3\rangle\rvert^2$	B(M1) (n.m.)^2	η [b])	Refs.	$\bar{\sigma}_\nu$ (10^{-45} cm^2)	Events/ day [c]) N_E
1	^{2}H(D_2O)	$1^+;0 \to 0^+;1$	2223		[g])			7.1	820
2	^{6}Li	$1^+;0 \to 0^+;1$	3563	5.06	5.37	0.084	[26])	3.4	300
3	^{7}Li	$\frac{3}{2}^- \to \frac{1}{2}^-$	478	1.78	2.48	0.29	[26])	26	2000
4	^{9}Be	$\frac{3}{2}^- \to \frac{5}{2}^-$	2429	0.52 [d])	0.81	0.36 [d])	[26,27])	1.2	260
5		$\to \frac{1}{2}^-$	2780	0.23	0.36		[26,27])	0.36	77
6	^{11}B	$\frac{3}{2}^- \to \frac{1}{2}^-$	2140	0.94 [d])	0.69	−0.07 [d])	[28])	3.0	660
7	^{13}C	$\frac{1}{2}^- \to \frac{3}{2}^-$	3684 [f])	0.73	1.22		[29])	0.44	77
8	^{19}F(MgF_2)	$\frac{1}{2}^+ \to \frac{3}{2}^+$	1554 [f])	0.05 [e])	< 0.12	≈0.55 [e])	[30])	0.29	32
9	^{23}Na	$\frac{3}{2}^+ \to \frac{5}{2}^+$	439	0.25	0.63	0.73	[31])	3.7	160
10		$\to \frac{3}{22}^+$	2982 [f])	0.15	0.25		[31])	0.19	8
11	^{25}Mg	$\frac{5}{2}^+ \to \frac{7}{2}^+$	1611	0.28	0.83	0.87	[31])	1.6	120
12	^{27}Al	$\frac{5}{2}^+ \to \frac{7}{2}^+$	2210	0.11	0.18	0.38	[31,32])	0.32	33
13		$\to \frac{5}{22}^+$	2734 [f])	0.05			[31])	0.084	9
14		$\to \frac{3}{22}^+$	2981	0.24	0.24	0.10	[31])	0.29	30
15	^{29}Si	$\frac{1}{2}^+ \to \frac{3}{21}^+$	1273	0.049	0.13	0.79	[31])	0.36	30
16		$\to \frac{3}{22}^+$	2426 [f])	0.31	0.40	0.23	[31])	0.70	59
17	^{31}P	$\frac{1}{2}^+ \to \frac{3}{21}^+$	1266	0.063	0.076	0.19	[31])	0.44	40
18		$\to \frac{1}{22}^+$	3134 [f])	0.062	0.18	0.87	[31])	0.064	6
19		$\to \frac{3}{22}^+$	3506 [f])	0.10	≧ 0.11	≦0.14	[31])	0.071	6
20	^{35}Cl($MgCl_2$)	$\frac{3}{2}^+ \to \frac{1}{2}^+$	1219	0.050	0.086	0.44	[31])	0.40	20
21		$\to \frac{3}{22}^+$	2694 [f])	0.074	0.055	−0.06	[31])	0.13	7
22		$\to \frac{5}{22}^+$	3003	0.062	0.090	0.31	[31])	0.073	4
23	^{43}Ca	$\frac{7}{2}^- \to (\frac{3}{2}^-)$	2069 [f])	0.13	0.21		[31])	0.45	17
24	^{55}Mn	$\frac{5}{2}^- \to \frac{3}{2}^-$	1529	0.13	0.22		[33])	0.74	100
25		$\to \frac{7}{2}^-$	1885 [f])	0.42	0.70		[33])	1.8	250
26		$\to (\frac{5}{2}^-, \frac{7}{2}^-)$	2199 [f])	0.13	0.21		[33])	0.39	55
27		$\to (\frac{3}{2}^-)$	2254	0.13	0.22		[33])	0.37	52
28		$\to \frac{1}{2}^-$	2565	0.11	0.19		[33])	0.23	32
29		$\to (\frac{7}{2}^-)$	3004	0.04	0.07		[33])	0.05	7
30	^{59}Co	$\frac{7}{2}^- \to \frac{9}{2}^-$	1189	0.46	0.77		[34])	3.6	570
31	^{63}Cu	$\frac{3}{2}^- \to \frac{1}{2}^-$	669	0.25	0.43		[35])	3.1	460
32		$\to \frac{5}{2}^-$	962	0.062	0.11		[35])	0.60	89
33	^{65}Cu	$\frac{3}{2}^- \to \frac{1}{2}^-$	770	0.40	0.67		[36])	4.6	660
34	^{79}Br	$\frac{3}{2}^- \to \frac{3}{24}^-$	833 [f])	0.29	0.48		[37])	3.1	130
35	^{81}Br	$\frac{3}{2}^- \to (\frac{5}{2}^-)$	767 [f])	0.21	0.35		[38])	2.5	100
36	^{89}Y	$\frac{1}{2}^- \to \frac{3}{2}^-$	1507	0.82	1.37		[39])	4.9	260
37	^{91}Zr	$\frac{5}{2}^+ \to \frac{3}{2}^+$	2042	0.13	> 0.22		[40])	0.50	37
38	^{93}Nb	$\frac{9}{2}^+ \to \frac{7}{2}^+$	744	0.13	0.21		[41])	1.6	150
39		$\to \frac{11}{2}^+$	979	0.14	0.23		[41])	1.4	130

[a]) See text for the explanation of the notation.

[b]) If the value of η is not given, the Gamow-Teller matrix element is calculated from the B(M1) value using $\eta = 0.41$.

[c]) With 1 m^3 of target and 2×10^{13}/sec/cm^2 antineutrino flux.

[d]) Shell model calculation [24]) of η used with the experimental B(M1) value.

[e]) Assuming a 0.01 % branching ratio or $\log ft = 5.1$, see ref. [25]).

[f]) Indicating that part of the γ-decay cascades.

[g]) See subsect. 2.5.

The results are shown in table 1. For ready reference we have assigned a numeral to each reaction in column 1. The target nuclei are listed in column 2. In column 3 the spin and parity, J^π, of the initial and final states are given. For reactions nos. 1 and 2 the isospins are also given, using the notation $J^\pi; T$. The initial and final isospins for all other reactions with $A < 40$ are both $\frac{1}{2}$. As will be made clear later, the isospin of the nuclear states in reactions with $A > 40$ need not be known for the computation of $\bar{\sigma}_\nu$. Therefore for these reactions the isospin is not given in table 1. Columns 4, 5, 6 and 9 list the excitation energy, $|g_A\langle\sigma\tau_3\rangle|^2$, B(M1) and the computed $\bar{\sigma}_\nu$, respectively. The source for experimental data are listed in column 8. The contents of column 7 and 10 will be explained in later sections.

3.2. RESULTS FOR DEUTERON

The neutrino disintegration of the deuteron is the only nuclear (ν, ν') reaction currently being studied experimentally [14]. Our result $\bar{\sigma}_\nu = 7.1 \times 10^{-45}$ cm^2, obtained by integrating the right-hand side of (16), is in agreement with the Ahrens and Lang result [22] 6.6×10^{-45} cm^2. Our 8% higher cross section is presumably due to the fact that the antineutrino spectrum [19] used in our calculation has slightly more

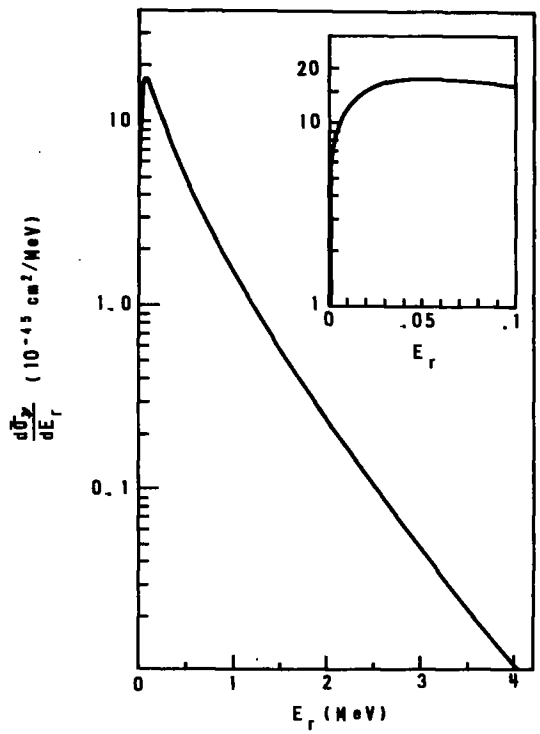

Fig. 5. Differential cross section for the ν-disintegration of the deuteron, as a function of the reduced proton-neutron energy E_r.

antineutrinos in the high-energy range than the older spectrum used by Ahrens and Lang. Significantly the present result is about 60% greater than the theoretical cross section of 4.4×10^{-45} cm^2 quoted by Gurr *et al.* [14]). Ahrens and Lang [22]) also obtained a result of 4.6×10^{-45} cm^2 when they used the much older spectrum of King *et al.* [23]), which has comparatively the least antineutrinos in the higher energy region.

The differential cross section $d\bar{\sigma}_w/dE_r$, as a function of proton-neutron relative kinetic energy E_r, is shown in fig. 5. For $E_r \gtrsim 100$ keV, $d\bar{\sigma}_w/dE_r$ decreases almost exponentially with increasing E_r. In fact more than 70% of the scattering takes place with $E_r < 500$ keV. This effect makes it difficult to measure the cross section by detecting the product protons as most of these particles would not be sufficiently energetic to escape the target assembly [14]).

3.3. RESULTS FOR NUCLEI WITH $A < 40$

Most reactions in this group are characterized by the availability of the experimental values of both $|g_A\langle\sigma\tau_3\rangle|^2$ and B(M1). These reactions are those, excepting reactions nos. 4, 6 and 8, for which a value of η, extracted from (14) using experimental $|g\langle\sigma\tau_3\rangle|^2$ and B(M1) values, appears in column 7 of table 1. For reactions nos. 4 and 6 the values of η were calculated using the p-shell model [24]), and the values of $|g_A\langle\sigma\tau_3\rangle|^2$ were calculated using (14). The $|g_A\langle\sigma\tau_3\rangle|^2$ value for reaction no. 8 was calculated in ref. [25]) also with the p-shell model. In fig. 4, $|g_A\langle\sigma\tau_3\rangle|^2$ is plotted against B(M1) for all reactions for which η is given in table 1. The strong correlation between $|g_A\langle\sigma\tau_3\rangle|^2$ and B(M1) is evident. As was discussed in subsect. 2.4, this establishes η as a useful empirical relation and shows that its mean value is 0.41.

The values of η for several reactions in the $A < 40$ category are not given in table 1. For these reactions $|g_A\langle\sigma\tau_3\rangle|^2$ is calculated from the experimental B(M1) value using (15). A common property of these reactions is that they all have a sizable branching ratio for decaying by emitting two γ-rays in cascade. In table 1 we indicate all such reactions by attaching a superscript f to the excitation energy.

The excitation energies of reactions nos. 3 and 9 do not satisfy criterion (iii) given at the beginning of this section. They are nevertheless included in table 1 because of the exceptionally large cross sections, especially for reaction no. 3.

Fig. 6 shows the cross section as functions of the initial neutrino energy [see eq. (5)] for ^{6}Li, ^{7}Li and some other nuclei. The arrows at the bottom of fig. 6 indicate the threshold energy applicable to the reactions indicated. The cross sections for ^{6}Li and ^{7}Li have previously been calculated by Donnelly *et al.* [25]) †. Our results for these two nuclei are in agreement with theirs.

A very noticeable feature in table 1 is that the transition in ^{6}Li has by far the largest $|g_A\langle\sigma\tau_3\rangle|^2$ value, reflecting the fact that (apart from the transition in ^{2}H)

† Note that in ref. [25]) cross sections *per nucleon* for ^{6}Li and ^{7}Li were plotted.

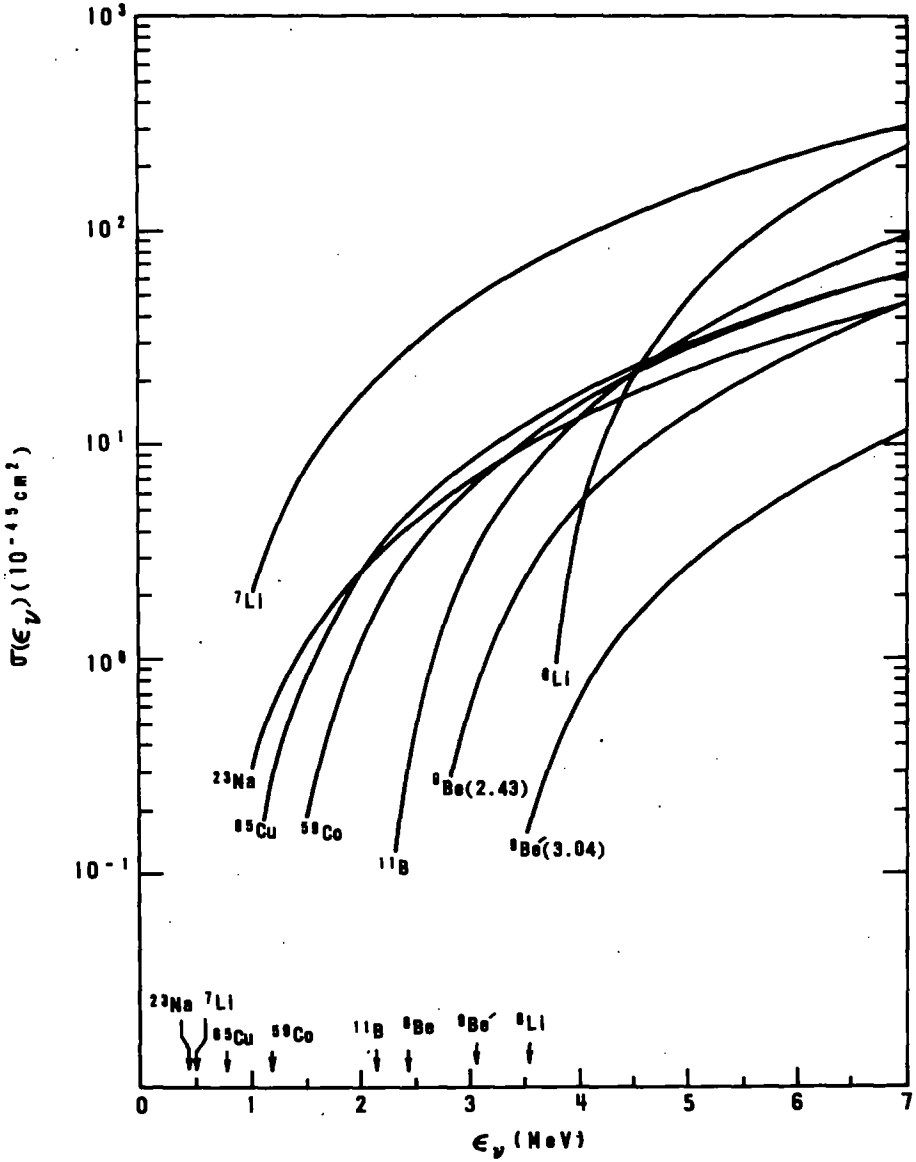

Fig. 6. The (ν, ν') cross sections for some targets, as functions of the antineutrino energy ε_ν. Arrows point to the threshold energies of the reactions indicated.

it is the only giant M1 transition. In the ^{7}Li transition a sizable fraction of the giant M1 strength in ^{6}Li is retained. In every other transition evidently only a small fraction of the total M1 strength from the ground state resides in the final state shown in table 1. Nevertheless ^{6}Li does not have the largest $\bar{\sigma}_\nu$. In fact the $\bar{\sigma}_\nu$ for ^{6}Li is approximately the same as that for reaction no. 9, which has a $|g_A\langle\sigma\tau_3\rangle|^2$ value twenty

times smaller than the value for ^{6}Li, but at the same time has a much lower excitation energy than ^{6}Li. This reflects the important role played by the neutrino spectrum in reducing the effective cross section at higher excitation energies.

3.4. RESULTS FOR NUCLEI WITH $A > 40$

For this group of reactions no experimental values of $|g_A\langle\sigma\tau_3\rangle|^2$ are available, and the $|g_A\langle\sigma\tau_3\rangle|^2$ values in table 1 are calculated from (15) using experimental B(M1) values. The list of nuclei in table 1 stops at $A = 93$ because for heavier nuclei even the experimental M1 strength (in the region $600 \lesssim \Delta \lesssim 4000$ keV) is generally not known with sufficient accuracy. It is interesting to note that many reactions in this category are predicted to have $\bar{\sigma}_\nu$ as large as that for ^{6}Li.

3.5. CONVERTING $\bar{\sigma}_\nu$ TO EVENTS PER DAY

Because of the extreme smallness of the (ν, ν') cross section, it is instructive to convert $\bar{\sigma}_\nu$ into number of events per day, N_E, for a given antineutrino flux impinging on a standard quantity of target. As a reference we use the nominal antineutrino flux [42]) (f) of $2\times10^{13}/\text{cm}^2\cdot\text{sec}$ available for experimental use at the 1800 MW Savannah River Reactor. In general about $2\times10^{17}\ \text{sec}^{-1}$ antineutrinos are produced in the reactor per MW of power generated. The flux external to the reactor will depend on the latter's geometry, size, etc. Expecting the most severe physical limitations are more likely to be those imposed upon the volume, V, of the target, we choose as a standard of quantity 1 m^3 of target. We thus have

$$N_E = \bar{\sigma}_\nu N\rho V f T/A = (\bar{\sigma}_\nu\rho/A)1.04\times10^{48}\ \text{events/day},$$

where N is Avogardro's number; ρ is the density (g/cm^3) of the target and T is the number of seconds per day. The result for N_E is listed in column 10 of table 1.

3.6. SUMMARY OF THE RESULTS

In table 2 we present the results of table 1 categorized in terms of possible detection schemes. Within each category the reactions are given in order of descending N_E value. Energies of the particles or γ-rays to be detected are given in column 4 of the table.

For reactions where particle detection is possible ^{2}H seems to be the most attractive target. On the other hand reaction no. 4, while having a smaller N_E value, offers the advantage of emitting more energetic neutrons.

Because the γ-ray background level below 1 MeV increases very rapidly with decreasing energy, reaction no. 3 (^{7}Li target), although having the largest N_E value, may be considered as a very unfavourable case on account of the low energy of the

TABLE 2

List of targets according to detection scheme

Detected particle	Reaction number	Target	Energy of particle(s) (keV)	Branching ratio (%) [a]	N_E [b]
proton	1	$^2H(D_2O)$	$\leqq$ 500		820
neutron	1	^2H	$\leqq$ 500		820
	4	^9Be	$\approx$ 680		260
γ	3	^7Li	478		2000
	33	^{65}Cu	770		660
	30	^{59}Co	1189		570
	31	^{63}Cu	669		460
	2	^6Li	3562		300
	36	^{89}Y	1507		260
	25	^{55}Mn	1885		250
	9	^{23}Na	440		160
2γ in	25	^{55}Mn	1759, 126	34	85
coincidence	8	$^{19}F(MgF_2)$	1357, 197	95	30
	26	^{55}Mn	1214, 984	43	23
	35	^{81}Br	538, 229	13	13
	15	^{29}Si	1273, 1153	13	8.1
	14	^{27}Al	1712, 1014	76	6.5
	34	^{79}Br	562, 271	5	6.5
	9	^{23}Na	2542, 440	42	3.3
	17	^{31}P	2240, 1266	38	2.5
	7	^{13}C	3088, 596	1.6	1.1
	21	$^{35}C(MgCl_2)$	1763, 931	14	1.0
n, α in	4	^9Be	$E_\alpha \approx$ 90, $E_n \approx$ 680	7.5	20
coincidence	5	^9Be	$E_\alpha \approx$ 110, $E_n \approx$ 990	$\leqq$ 100	$\approx$ 62

[a]) Branching ratio is 100 % when not given.
[b]) Events/day, see table 1.

γ-ray that it emits. Conversely, because of the relative high energy † of the γ-ray emitted ^6Li may be considered as a more favorable case.

The signal to noise ratio could become significantly greater when the reaction signature is a pair of cascade γ-rays. Among reactions where this is the case no. 26 could be considered as the most attractive, since it has a reasonably large N_E value and at the same time both of its γ-rays have $E_\gamma \gtrsim 1$ MeV. Reactions nos. 25 and 8, although with N_E values larger than that for no. 26, are probably not as practicable, again on account of the very low energy of one of the γ-rays emitted in each reaction.

† In fact the energy 3562 keV is above the energies of practically all γ-rays due to natural radioactivity.

4. Summary

We have pointed out that the measurement of cross sections for low-energy inelastic neutrino scattering by nuclei is the most direct test of the Salam-Weinberg theory as regards the axial vector component of the nuclear neutral current. In this paper the (ν, ν') cross section $(\bar{\sigma}_\nu)$ integrated over the reactor antineutrino spectrum is presented in a form that can be evaluated immediately whenever the neutral, or charge non-changing, Gamow-Teller nuclear matrix element $g_A\langle\sigma\tau_3\rangle$ is known [eq. (8)]. This matrix element is related to the corresponding β-decay Gamow-Teller matrix element by a rotation in isospin [eq. (10)].

Using these relations and available experimental data on nuclear Gamow-Teller transitions, we calculated $\bar{\sigma}_\nu$ for many transitions in p-shell and sd shell nuclei, where $A < 40$. In these transitions we also observed a strong correlation between measured values of $|g_A\langle\sigma\tau_3\rangle|^2$ and of B(M1) which is summarized in eq. (15). We were able to use this correlation and available experimental data on B(M1) to calculate $\bar{\sigma}_\nu$ for many additional transitions, mostly in nuclei with $A > 40$, where experimental data on the relevant β-decays are not available. Using the most recent spectrum for reactor antineutrinos, we also calculated a new value of $\bar{\sigma}_\nu$ for the ν-disintegration of ^{2}H. These results are given in table 1.

In table 2 the reactions for which $\bar{\sigma}_\nu$ was calculated are categorized in terms of possible detection schemes. For particle detection the neutron signatures of reactions nos. 1 and 4, with ^{2}H and ^{9}Be respectively as targets, present the most promising possibilities. An experiment on reaction no. 1 has been underway for some time [14]. We note that reaction no. 2 (^{6}Li target) is the most promising experiment for which a single γ-ray is detected and reaction no. 26 (^{55}Mn target) is the most promising in which two γ-rays are observed in coincidence.

We thank T. W. Donnelly for a useful communication.

Appendix A

CROSS SECTION FOR (ν, ν') ON A NUCLEUS

The differential cross section for the inelastic neutrino scattering which induces the nuclear transition $|i\rangle \to |f\rangle$ is

$$d\sigma_{i\to f} = \frac{1}{v_i}\frac{m_\nu^2}{\varepsilon_i\varepsilon_f}\frac{1}{2J_i+1}\frac{d\boldsymbol{p}_f}{(2\pi)^3}\frac{d\boldsymbol{P}_f}{(2\pi)^3}(2\pi)^4\delta^4(p_i+P_i-p_f-P_f)\sum{}'|\mathscr{L}_{\nu N}|^2, \quad \text{(A.1)}$$

where [†] $v_i = c = 1$ is the initial velocity of the neutrino; p_i (p_f) and P_i (P_f) are respectively the initial (final) four-momenta of the neutrino and the nucleus; $\varepsilon_{i,f} = |\boldsymbol{p}_{i,f}|$; J_i is the initial nuclear spin; and $\sum'$ sums over the nuclear magnetic substates and the

[†] We use $c = \hbar = 1$, and in general the conventions of Bjorken and Drell [43]).

neutrino spin orientations. The factor of neutrino mass squared, m_ν^2, appears because we use the conventional normalization for Dirac wave functions [43]). It will be cancelled by an identical factor contained in $|\mathscr{L}_{\nu N}|^2$.

According to Weinberg [10]), the lowest-order neutrino-nuclear Lagrangian is

$$\mathscr{L}_{\nu N} = \sqrt{\tfrac{1}{2}} G_w j_\nu^\mu \mathscr{J}_\mu, \tag{A.2}$$

where

$$j_\nu^\mu = \bar{u}_\nu(p_f)\gamma^\mu(1 \pm \gamma_5)u_\nu(p_i) \tag{A.3}$$

is the neutrino or antineutrino (+ or − sign) current and

$$\mathscr{J}_\mu(q) = \langle f|e^{-iq\cdot r}\hat{\mathscr{J}}_\mu^{(0)}|i\rangle. \tag{A.4}$$

Here $\mathscr{J}_\mu$ is the nuclear matrix element of the current operator $\hat{\mathscr{J}}_\mu^{(0)}$ for momentum transfer $q = p_i - p_f$. Summing over the neutrino spins we have

$$\begin{aligned} m_\nu^2 \sum_{s_i s_f} |\mathscr{L}_{\nu N}|^2 &= \tfrac{1}{2} G_w^2 \mathscr{J}_\mu \mathscr{J}_\sigma^* \tfrac{1}{4} \operatorname{Tr}[\gamma^\mu(1 \pm \gamma_5) p_i (1 \mp \gamma_5)\gamma^\sigma p_f] \\ &= G_w^2 \mathscr{J}_\mu \mathscr{J}_\sigma^* (p_i^\mu p_f^\sigma + p_i^\sigma p_f^\mu - \delta_{\mu\sigma} p_i \cdot p_f \pm i\varepsilon_{\mu\beta\sigma\delta} p_i^\beta p_f^\delta) \\ &= \tfrac{1}{2} G_w^2 \{(Q\cdot\mathscr{J})(Q\cdot\mathscr{J}^*) - (q\cdot\mathscr{J})(q\cdot\mathscr{J}^*) + \tfrac{1}{2}(q^2 - Q^2)\mathscr{J}\cdot\mathscr{J}^* \\ &\quad \pm i\varepsilon_{\mu\beta\sigma\delta}\mathscr{J}^\mu Q^\beta \mathscr{J}^{\sigma *} q^\delta\}, \end{aligned} \tag{A.5}$$

where $q = p_i - p_f$, $Q = p_i + p_f$ and $\varepsilon_{\alpha\beta\gamma\delta}$ is the totally antisymmetric fourth-order tensor with $\varepsilon_{1234} = 1$. Choosing q to be the direction of quantization we write, for any four vector A,

$$A\cdot\mathscr{J} \equiv A_4\rho - A\cdot J = A_4\rho - (A\cdot q/|q|)J_0 + \sum_{k=\pm 1} A_k J_{-k}, \tag{A.6}$$

where $\mathscr{J} = (J_4, J) \equiv (\rho, J)$ and $J_0, J_{\pm 1}$ are the three polar components of J. We now multipole expand ρ, J_0 and $J_{\pm 1}$ in the conventional manner [17]),

$$\begin{aligned} \rho(q) &= -(4\pi)^{\frac{1}{2}} \sum_{\lambda=0}^{\infty} a_{\lambda 0} M_\lambda(q), \\ J_0(q) &= -(4\pi)^{\frac{1}{2}} \sum_{\lambda=0}^{\infty} a_{\lambda 0} L_\lambda(q), \\ J_{\pm 1}(q) &= -(2\pi)^{\frac{1}{2}} \sum_{\lambda=1}^{\infty} a_{\lambda\pm 1}[-T_\lambda^{el}(q) \pm T_\lambda^{mag}(q)], \end{aligned} \tag{A.7}$$

with

$$a_{\lambda k} \equiv (-i)^\lambda (2\lambda+1)^{\frac{1}{2}} \langle J_i M_i \lambda k | J_f M_f \rangle. \tag{A.8}$$

Here $M_\lambda(q)$, etc., are short-hand notations for the reduced nuclear multipole matrix

elements

$$M_\lambda(q) \equiv \langle J_f \| M_\lambda(q) \| J_i \rangle, \tag{A.9}$$

etc. Substituting (A.6)–(A.9) into (A.5) and (A.2) and after further straightforward reductions we obtain eq. (2) of subsect. 2.1.

Appendix B

NEUTRINO DISINTEGRATION OF THE DEUTERON

The final state of this reaction has three particles, one more than the reactions discussed in the last section. Instead of (5) of subsect. 2.1, we now have

$$\frac{d\sigma(\varepsilon_\nu)}{dE_r} = \frac{G_w^2}{4\pi^3} M^{\frac{1}{2}} E_r^{\frac{1}{2}} (\varepsilon_\nu - B - E_r)^2 |g_A \langle {}^3S_1; 0 \| \sigma\tau_3 \| {}^1S_0(E_r); 1 \rangle|^2, \tag{B.1}$$

where E_r is the reduced, or relative kinetic energy of the final neutron and proton, and M is the nucleon mass. Here $B = 2.22$ MeV and $|{}^3S_1; 0\rangle$ are respectively the binding energy and the wave function of the deuteron, and $|{}^1S_0(E_r); 1\rangle$ is the wave function of the proton-neutron singlet continuum. In the zero effective range approximation [44] $\langle r|{}^3S_1; 0\rangle = (\kappa/2\pi)^{\frac{1}{2}} e^{-\kappa r}/r$, where $\kappa = (MB)^{\frac{1}{2}}$, and $\langle r|{}^1S_0(E_r); 1\rangle = \sin(pr + \delta_s)/pr$, where $p = (ME_r)^{\frac{1}{2}}$ and $\cot \delta_s = -1/a_s p$, $a_s = -23.7$ fm being the singlet scattering length. This approximation has a 2% error for the $\langle \sigma\tau_3 \rangle$ matrix element [22]) [but a $\approx 70\%$ error for the $\langle r \rangle$ matrix element [45])]. We then have

$$|\langle {}^3S_1; 0 \| \sigma\tau_3 \| {}^1S_0(E_r); 1 \rangle|^2 = \frac{8\pi B^{\frac{1}{2}} (E_s^{\frac{1}{2}} + B^{\frac{1}{2}})^2}{M^{\frac{1}{2}} (E_s + E_r)(B + E_r)^2}, \tag{B.2}$$

where $E_s = (\hbar c)^2/a_s^2 M = 0.0738$ MeV. Substituting (B.2) into (B.1) and integrating over the reactor neutron spectrum we obtain (17) of subsect. 2.5.

References

1) F. Reines and C. L. Cowan, Phys. Rev. **92** (1953) 830
2) G. Danby *et al.*, Phys. Rev. Lett. **9** (1962) 36
3) M. M. Block *et al.*, Phys. Lett. **12** (1964) 281
4) L. M. Lederman, Am. J. Phys. **38** (1970) 129
5) J. Schwinger, Ann. of Phys. **2** (1957) 407
6) S. L. Glashow, Nucl. Phys. **22** (1961) 579
7) P. W. Higgs, Phys. Rev. **149** (1966) 1156
8) A. Salam and J. C. Ward, Phys. Lett. **13** (1964) 168;
   A. Salam, in Elementary particle physics, ed. N. Svarthom (Almqvist and Wiksells, Stockholm, 1968) p. 367
9) S. Weinberg, Phys. Rev. Lett. **19** (1967) 1264; Rev. Mod. Phys. **46** (1974) 255
10) S. Weinberg, Phys. Rev. **D5** (1972) 1412
11) F. J. Hassert *et al.*, Phys. Lett. **46B** (1973) 121
12) M. J. Counihan, A bibliography of experimental neutrino physics, Rutherford Laboratory report RL-76-133/A (1976)

13) L. L. Lewis *et al.*, Phys. Rev. Lett. **39** (1977) 795;
P. E. G. Baird *et al.*, Phys. Rev. Lett. **39** (1977) 798
14) H. S. Gurr, F. Reines and H. W. Sobel, Phys. Rev. Lett. **33** (1974) 179
15) M. Gari and J. Schlitter, in Interaction studies in nuclei, ed. H. Jochim and B. Ziegler (North-Holland, Amsterdam, 1975) p. 105
16) S. S. Gershtein, N. van Hieu and R. A. Bramzhyan, JETP (Sov. Phys.) **16** (1963) 1097
17) J. S. O'Connell, J. W. Donnelly and J. D. Walecka, Phys. Rev. **C6** (1972) 719;
T. W. Donnelly and J. D. Walecka, Nucl. Phys. **A274** (1976) 368 and references therein;
J. D. Walecka, in Muon physics, vol. 2, ed. V. W. Hughes and C. S. Wu, p. 113
18) M. M. Nagels *et al.*, Nucl. Phys. **B109** (1976) 1
19) F. T. Avignone, Phys. Rev. **D2** (1970) 2609
20) D. H. Wilkinson, Nature **257** (1975) 189;
J. C. Hardy and I. S. Towner, Nucl. Phys. **A254** (1975) 221;
S. Raman, T. A. Walkiewicz and H. Behrens, Atomic Data and Nucl. Data Tables **16** (1975) 451
21) M. Chemtob and M. Rho, Nucl. Phys. **A163** (1971) 1
22) T. Ahrens and T. P. Lang, Phys. Rev. **C3** (1971) 979 and references therein
23) H. R. Brewer, R. W. King and R. A. Mears, quoted in ref. [22]);
R. W. Ring and J. F. Perkins, Phys. Rev. **170** (1958) 930
24) I. S. Towner, private communication
25) T. W. Donnelly, D. Hitlin, M. Schwartz, J. D. Walecka and S. J. Wiesner, Phys. Lett. **49B** (1974) 8
26) A. Ajzenberg-Selove and T. Lauritsen, Nucl. Phys. **A227** (1974) 1
27) L. W. Fagg, Rev. Mod. Phys. **47** (1975) 683
28) F. Ajzenberg-Selove, Nucl. Phys. **A248** (1975) 1
29) F. Ajzenberg-Selove, Nucl. Phys. **A268** (1976) 1
30) F. Ajzenberg-Selove, Nucl. Phys. **A190** (1972) 1
31) P. M. Endt and C. van der Leun, Nucl. Phys. **A214** (1973) 1
32) F. M. Mann, H. S. Wilson and R. W. Kavanagh, Nucl. Phys. **A258** (1976) 341
33) D. C. Kocher, Nucl. Data Sheets **18** (1976) 463
34) H. J. Kim, Nucl. Data Sheets **17** (1976) 485
35) R. L. Auble, Nucl. Data Sheets **14** (1975) 119
36) R. L. Auble, Nucl. Data Sheets **16** (1975) 351
37) P. P. Urone, D. C. Kocher, Nucl. Data Sheets **15** (1975) 257
38) J. F. Lemming, Nucl. Data Sheets **15** (1975) 137
39) D. C. Kocher, Nucl. Data Sheets **16** (1975) 445
40) G. A. Gill, R. D. Gill and G. A. Jones, Nucl. Phys. **A224** (1974) 152
41) D. C. Kocher, Nucl. Data Sheets **8** (1972) 527
42) F. Reines, H. S. Gurr and H. W. Sobel, Phys. Rev. Lett. **37** (1976) 315
43) J. D. Bjorken and S. D. Drell, Relativistic quantum mechanics (McGraw-Hill, NY, 1965)
44) L. Hulthén and M. Sugawara, in Handbuch der Physik, vol. 39, ed. S. Flügge (Springer, Berlin, 1957) p. 1
45) H. C. Lee and F. C. Khanna, Phys. Rev. **C14** (1976) 1306